



**University of Dundee**

**A thermoanalytical, X-ray diffraction and petrographic approach to the forensic assessment of fire affected concrete in the United Arab Emirates**

Alqassim, M. A.; Jones, M. R.; Berlouis, L. E. A.; Nic Daeid, N.

*Published in:*  
Forensic Science International

*DOI:*  
[10.1016/j.forsciint.2016.03.015](https://doi.org/10.1016/j.forsciint.2016.03.015)

*Publication date:*  
2016

*Licence:*  
CC BY-NC-ND

*Document Version*  
Peer reviewed version

[Link to publication in Discovery Research Portal](#)

*Citation for published version (APA):*

Alqassim, M. A., Jones, M. R., Berlouis, L. E. A., & Nic Daeid, N. (2016). A thermoanalytical, X-ray diffraction and petrographic approach to the forensic assessment of fire affected concrete in the United Arab Emirates. *Forensic Science International*, 264, 82-88. <https://doi.org/10.1016/j.forsciint.2016.03.015>

**General rights**

Copyright and moral rights for the publications made accessible in Discovery Research Portal are retained by the authors and/or other copyright owners and it is a condition of accessing publications that users recognise and abide by the legal requirements associated with these rights.

- Users may download and print one copy of any publication from Discovery Research Portal for the purpose of private study or research.
- You may not further distribute the material or use it for any profit-making activity or commercial gain.
- You may freely distribute the URL identifying the publication in the public portal.

**Take down policy**

If you believe that this document breaches copyright please contact us providing details, and we will remove access to the work immediately and investigate your claim.

# ATHERMOANALYTICAL, X RAY DIFFRACTION AND PETROGRAPHIC APPROACH TO THE FORENSIC ASSESSMENT OF FIRE AFFECTED CONCRETE IN THE UNITED ARAB EMIRATES

**M.A. Alqassim**

[mamaalqassim@dundee.ac.uk](mailto:mamaalqassim@dundee.ac.uk)

CAHID, School of Science and Engineering, University of Dundee, Dow Street, Dundee DD15EH, Scotland, UK.

Corresponding Author. Tel.: + 44(0) 1382 388933; fax: + 44 (0)1382 386817

**M.R. Jones**

[m.r.jones@dundee.ac.uk](mailto:m.r.jones@dundee.ac.uk)

Concrete Technology Unit, Division of Civil Engineering, School of Science and Engineering, University of Dundee, Dundee DD14HN, Scotland, UK.

**L.E.A Berlouis**

[l.berlouis@strath.ac.uk](mailto:l.berlouis@strath.ac.uk)

WESTCHEM, Department of Pure and Applied Chemistry, University of Strathclyde, 295 Cathedral Street, Glasgow G11XL, Scotland, UK.

**N. Nic Daeid**

[n.nicdaeid@dundee.ac.uk](mailto:n.nicdaeid@dundee.ac.uk)

CAHID, School of Science and Engineering, University of Dundee, Dow Street, Dundee DD15EH, Scotland, UK.

## **Keywords**

Forensic investigation; Concrete; Fire; Thermal Analysis; X-ray Diffraction; Colour Change.

## **Highlights**

- This work studies the application of thermogravimetric analysis, differential scanning calorimetry, X-ray diffraction and petrography as tools for revealing the thermal history on concrete structures.
- Some chemical reactions are irreversible. The absence of certain minerals in the concrete matrix is an indicator of the maximum temperature reached.

- Other reactions can be reversible, particularly the dehydroxylation of Portlandite. The thermal history can still be determined though by comparing the onset temperature of reformed components with Portlandite in non-previously heated samples.

## Abstract

For most fires, forensic investigation takes place well after building materials have cooled and knowledge of the structural damage due to heat exposure can reveal the temperature reached during an incident. Recently, there have been significant changes in the types and hence characteristics of cementitious materials used in the United Arab Emirates. Few studies focus on the application of thermo-analytical, X-ray diffraction and petrographic techniques on newly developed structures and this work aims to address this deficiency by utilising a series of parametric laboratory-based tests to assess the effects of heat on hardened concrete. Specimens were made with a design mix typically used for low-rise residential homes and storage facilities. The key constituents were: Portland cement (PC), crushed gabbro stone and dune sand with water/cement ratios of 0.4-0.5. Portland cement substitutes included ground granulated blast-furnace slag (GGBS), and silica fume (SF) at replacement percentages of up to 50% and 4%, respectively. The concrete cubes of 100-mm size were produced and standard cured to 28 days and then exposed to heat inside an electric furnace with pre-determined temperature regimes of 150°C, 300°C, 600°C and 900°C. Petrographic examination was utilised to compare the discolouration of the cooled concrete. Data derived from thermogravimetric analysis (TGA) and differential scanning calorimetry (DSC) are reported in order to assess the usefulness of these techniques in fire scene investigation to differentiate between these temperature regimes. The results from the TGA indicate that the majority of the percentage weight loss for all the mixtures occurred in the range 650-700°C, which corresponds to the decarbonation of calcium carbonate, mainly from the aggregates. The endothermic DSC peak at 70-120°C relates to the loss of evaporable water. Since both of these reactions are irreversible, this information can help fire investigators estimate the temperature history of concrete after exposure to fire. On the other hand, the portlandite in the cement matrix dehydroxylates at 450-550°C but then reforms as the concrete cools. The onset temperature for the dehydroxylation of the reformed mineral is always lower than in virgin samples and its enthalpy furthermore depends strongly on the thermal history of the portlandite. Thus, this feature can be used to establish the temperature to which the material was exposed to during a fire incident.

## 1. Introduction

A series of physical, mechanical and mineralogical changes take place in the concrete matrix during exposure to sudden high thermal stress[1]. Certain properties, including strength, surface colour and weight loss, have already been used by investigators as potential indicators of the extent of fire during scene reconstruction of incidents that have happened in structural dwellings[2]. Therefore, understanding the reactions that occur, particularly in the cement paste part of the concrete, provides additional valuable information. Some of these reactions are irreversible while others might be reversible during the cooling following a fire[3]. Both types of changes within the concrete structure have the potential to be used as indicators of the maximum temperature to which the material has been exposed[4]. As such their detection and evaluation through a combination of thermo-analytical, X-ray diffraction and petrographic techniques may be useful in providing an objective measure of the exposure temperature.

Colour change at the concrete surface and within cross-sections adds helpful information relating to the maximum temperature to which the material was exposed, as most discolouration is associated with oxidation and decarbonation reactions that take place in both the aggregates and the cement mortar[5-8]. The main characteristics explored in this work are moisture loss from the decomposition of the calcium silicate hydrate (C-S-H), the transformation of the portlandite ( $\text{Ca}(\text{OH})_2$ ), the oxidation of iron hydroxides ( $\text{Fe}(\text{OH})_2$ ) and the decarbonation of calcium carbonates ( $\text{CaCO}_3$ )[9]. The following shows the temperature ranges over which each reaction generally occurs[10, 11]:

- 70°C–200°C: the dissociation of ettringite (calcium sulfoaluminate) and gypsum (calcium sulfate dihydrate) in the cement paste
- 180°C–300°C: loss of bound water from the decomposition of the C-S-H gel
- 300°C–350°C: oxidation of iron hydroxides in aggregate and cement paste
- 380°C–500°C: dehydroxylation of  $\text{Ca}(\text{OH})_2$  as  $\text{CaO}$  and  $\text{H}_2\text{O}$
- 600°C: quartz transformation causing radial cracks around aggregate particles
- 650°C–800°C: decomposition of the dehydrated  $\text{CaCO}_3$  as  $\text{CaO}$  and  $\text{CO}_2$

Thus, from the above, the absence of  $\text{CaCO}_3$  in the cement paste formulation would be an indicator that the temperature had exceeded  $800^\circ\text{C}$ .  $\text{Ca}(\text{OH})_2$  reforms during the cooling down of concrete, and although this reaction is reversible, the thermal history can still be determined by comparing the onset temperature at which the reformed compound decomposes and the enthalpy associated with this event, which are usually dissimilar to the untreated material [12-14].

## 2. Materials and Methods

A total of three different concrete mixtures were prepared. The concrete mixture that contained 100% PC using 0.4 water/cement ratio was considered as the control mixture. The second mixture contained the same type of binder but with a higher water content in order to study additional free moisture effects on thermal resistance. The final concrete mixture contained GGBS and SF as substitute cementitious materials. The reason for choosing those two materials is that they are the most common cement substitutes used within the UAE [15, 16]. The replacement percentages of GGBS and SF were 50% and 4%, respectively.

The type of PC was CEM I 42.5 N, which is the most commercially available cement in the UAE. The SF was provided in a densified slurry form consisting of 48-50% water. The GGBS conformed to BS EN 15167. The type of coarse aggregate (10/20 and 4/10) employed was crushed gabbro stone from Fujairah, UAE. The fine aggregates were from two different sources: gabbro (0/4) and dune sand with a maximum particle size of 0.6 mm from Al Ain Desert. The physical properties and sieve analysis results for the aggregates are provided in Table 1. The mixing water satisfied the limits set by BS EN 1008, and was directly provided from the laboratory. The superplasticizer (SP) was polycarboxylate ethers with 34%–36% solid content and density of  $1081 \text{ kg/m}^3$ .

The concrete mixtures were prepared in the Civil Engineering Laboratories at the University of Dundee and their compositions are presented in Table 2. The water/cement ratio ranged from 0.4 to 0.5. All concrete mixtures were prepared by adding SP to achieve slump class S4. In the UAE, the typical cement content for C40 strength class using a maximum 20-mm aggregate is in the range  $360\text{--}400 \text{ kg/m}^3$ . Therefore, the control cement volume used for this study was set at an average value ( $380 \text{ kg/m}^3$ ). Lower cement contents are used on rare occasions but are usually avoided owing to durability issues, specifically when PC only is applied without any replacements. The aggregate made up 78% of the total volume of the

concrete. Additionally, Mix C contained GGBS and SF. The cement types for this study were: CEM I and CEM III/A. Table 3 presents the oxide content of the cements.

**Table 1: Physical Properties of the Aggregates**

Physical Properties	Gabbro Aggregate			Sand
	10/20	4/10	0/4	0/0.6
<b>Water Absorption (%)</b>	0.6	0.7	1.2	0.8
<b>Bulk Specific Gravity (OD)</b>	2.86	2.84	2.64	2.62
<b>Bulk Specific Gravity (SSD)</b>	2.88	2.86	2.67	2.64
<b>Apparent Specific Gravity</b>	2.91	2.90	2.73	2.68
<b>Particle Size Distribution, percentage passing by mass</b>				
<b>20 mm</b>	100	-	-	-
<b>14 mm</b>	98	100	-	-
<b>10 mm</b>	3	59	100	-
<b>4 mm</b>	-	5	98	-
<b>2.36 mm</b>	-	-	67	-
<b>1.18 mm</b>	-	-	42	-
<b>0.6 mm</b>	-	-	27	100
<b>0.3 mm</b>	-	-	17	54
<b>0.15 mm</b>	-	-	11	47
<b>0.075 mm</b>	-	-	4	2

**Table 2: Mix Proportions**

Mix	Cementitious Materials (kg/m <sup>3</sup> )			Free Water (L)	Aggregate (kg/m <sup>3</sup> )		SP (%wt. of cement content)
	PC	GGBS	SF		Fine	Coarse	
A	380	-	-	152	927	1080	0.70
B	380	-	-	190	880	1022	0.52
C	175	190	30 <sup>a</sup>	152	915	1075	0.70

<sup>a</sup> SF contains 48-50% water by unit weight.

**Table 3: Main Oxide Constituents of the Cements\***

Composition(%mass)	Cement Type		
	PC	SF	GGBS
<b>SiO<sub>2</sub></b>	21.6	<b>91.4</b>	32.9
<b>Al<sub>2</sub>O<sub>3</sub></b>	5.5	1.2	13.6
<b>Fe<sub>2</sub>O<sub>3</sub></b>	3.6	0.5	0.9
<b>CaO</b>	<b>65.7</b>	1.2	<b>43.4</b>
<b>MgO</b>	1.6	0.8	4.6
<b>SO<sub>3</sub></b>	2.0	1.8	1.7

\* determined by X-Ray Fluorescence.

100-mm cube samples were made and standard cured for 7, 28 and 90 days and then subjected to compressive strength tests. For the investigation of the physical and mechanical effect of high temperature exposure, concrete prisms of 300-mm long and 75-mm

cross-sections were produced and standard cured then in air at laboratory ambient temperature for another two months while waiting for the heat treatment. The beams were then wet sawn to four equal 75-mm cubes and consequently heated at a rate of 10°C/min in a Carbolite OAF chamber furnace up to various predetermined temperature regimes (150°C, 300°C, 600°C and 900°C). Each sample was kept at the steady-state heat peak for four continuous hours and was then left to cool down in the furnace to the ambient temperature. The sample was then stored in a desiccator. The average carbonation depth of the non-heated concrete at the same age of heat exposure is shown in Table 5.

**Table 4: Carbonation Depth at the Age of Testing by Phenolphthalein Method**

Mixture	A	B	C
Carbonation Depth (mm)	0.0	0.5	1.5-2.0

The samples to be analysed were collected from the inner cores of the crushed specimens. The material was ball milled until a grain size of 80µm was obtained. Although earlier studies focused only on cement paste since aggregates tend to mask certain features, the presence of aggregates does not necessarily affect the conclusions reached from the analyses [17]. This is also important for the practical application of these measurements, as real-world samples will inevitably include aggregate dust.

Thermogravimetric analysis (TGA) was performed using a Perkin Elmer TGA7 with a TAC7/DX controller linked to a personal computer for data logging and control. The temperature of the furnace was programmed to rise at a constant rate of 10°C/min up to 900°C. The tests were performed under an air flow of 30 mL/min. The amount of material used for the tests was weighed with an analytical balance with an accuracy of ±0.1 mg. Samples of nearly 18–24 mg were taken from a larger batch of well-mixed powder (approximately 50 g), so as not to introduce bias into our measurements. Similar work using the same technique was previously reported by Harmathy [17], Handoo *et al.* [18] and Alarcon-Ruiz *et al.* [12].

The DSC employed was an HP DSC827 Mettler Toledo instrument controlled by the STAR software. It has two aluminium crucibles, one of which was empty and served as the reference pan and the other contained the sample to be analysed. In each experiment, the weight of the powder sample used was in the range 12–28 mg and a heating rate of 10 K/min was applied



up to 600°C. Powder X-ray diffraction data was collected using a Bruker D5000 diffractometer operating in reflection mode and using Cu K $\alpha$  radiation ( $\lambda=1.54056\text{\AA}$ ). Data was collected at ambient temperature in the range 5° to 50° in 2 $\theta$ .

Repetitive analysis (n=4) were performed for each concrete mix for all measurements.

### 3. Results and Discussion

The standard cube strength data is given in Table 4 and reflect the use of an equal water/cement ratio for all mixes. In addition, Table 4 summarises the effect of the heat cycle on the 75-mm cube specimens.

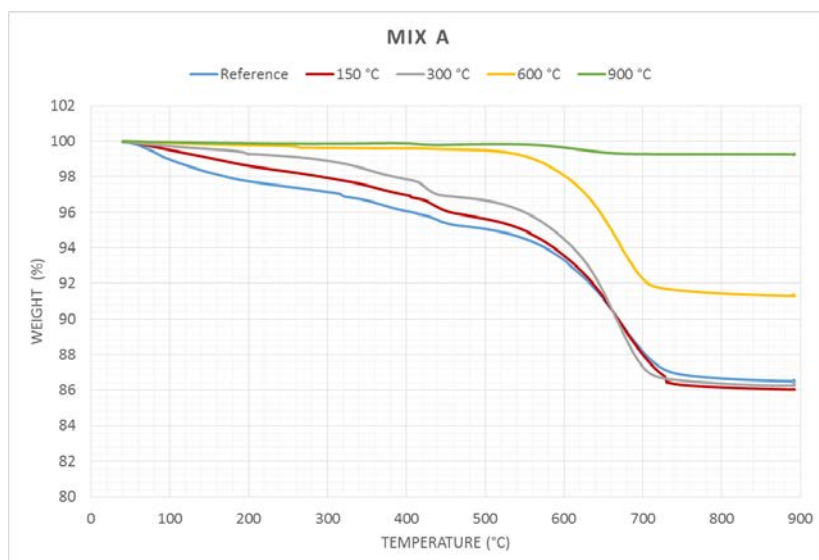
**Table 5: Strength Gain vs Curing Time and Relative Strength (%)**

Compressive Strength (MPa)	Mix		
	A	B	C
7 days	42.9	33.4	26.7
28 days	50.5	42.7	43.4
90 days	65.1	53.9	53.5
Treatment Temperature (°C)	Relative Strength (%)		
150	88.5	95.6	102.9
300	120.0	117.7	119.3
600	93.4	98.0	119.3
900	18.0	20.6	19.3

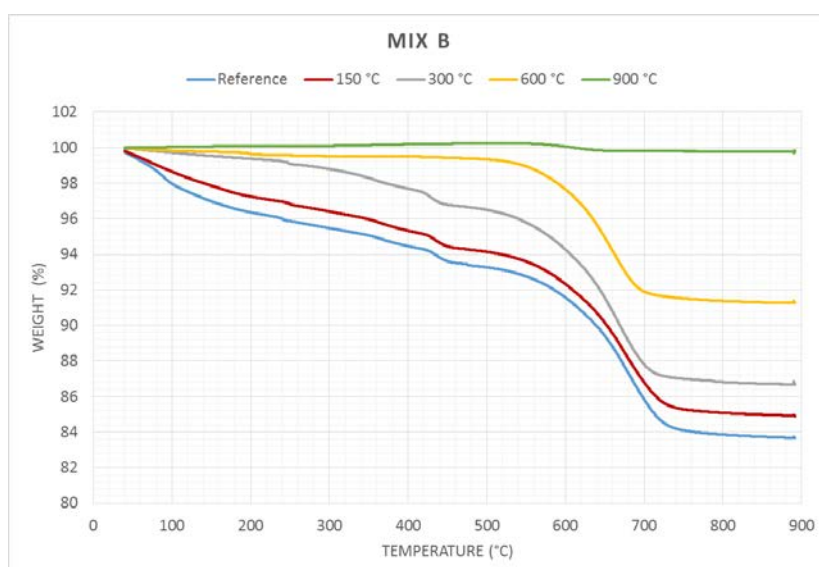
From the results revealed in Table 4, Mix A achieved the highest average strength gain over time. The strengths for Mixes B and C followed similar trends up to 90 days, although Mix C initially had the lowest 7-day strength. The residual strengths of the concrete were measured 24 hours after the heating periods. Concrete containing GGBS and SF exhibited better heat resistance up to 600°C. However, beyond that temperature, there was a dramatic loss in strength for all mixes.

#### 3.1 Thermogravimetric Analysis (TGA)

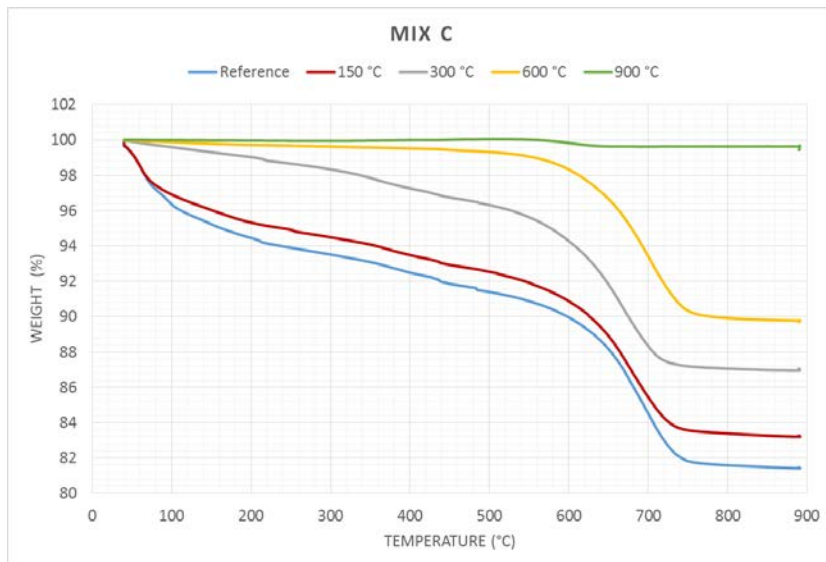
The TGA data from the samples are presented in Figures 1-3.



**Figure 1: TGA for Mix A**



**Figure 2: TGA for Mix B**



**Figure 3: TGA for Mix C**

The major weight loss observed in all mixtures occurred as a direct result of the decarbonation of  $\text{CaCO}_3$ , mainly from the aggregates, which in isolation takes place at temperatures beyond than  $700^\circ\text{C}$ [19]. The onset temperature of this reaction is reduced to around  $600^\circ\text{C}$  if it is in contact with quartz (present in dune sand), which reacts with the calcium oxide as it forms[20]. This reaction is clear in all pre-heated specimens apart from those that were previously heated to  $900^\circ\text{C}$ . The latter exhibited a weight loss of only 0.3%–0.7%.

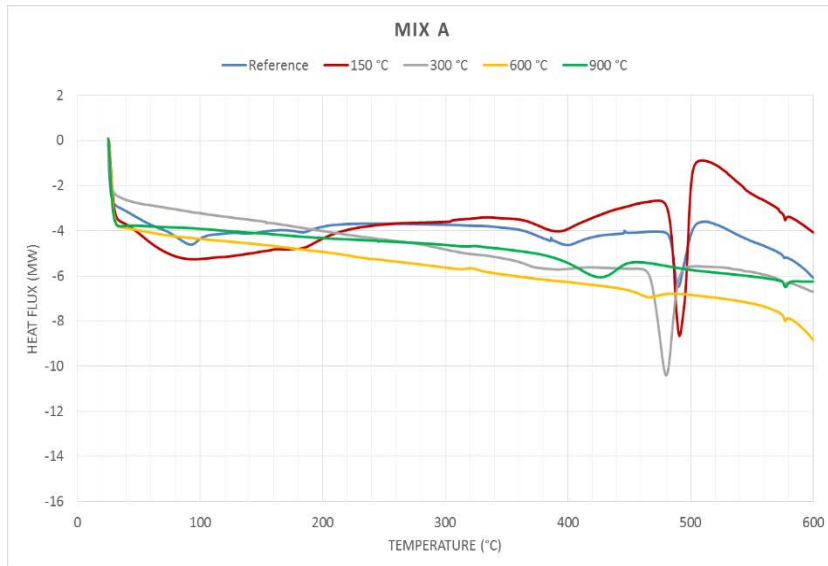
The highest total weight loss (19%) was found for Mix C and Mix A had the least overall weight loss (16.5%). Conversely, specimens from Mix A which were pre-heated up to  $900^\circ\text{C}$  had the highest weight loss when compared to Mix B and Mix C.

At  $300^\circ\text{C}$ , the reference sample of Mix C revealed the highest weight loss attributed to the dissociation of the C-S-H gel (about 6.5%), even though its initial moisture content was less than that of Mix B. Samples pre-heated to  $300^\circ\text{C}$  had a similar percentage weight loss across all Mixes at that point. For samples pre-heated to  $600^\circ\text{C}$  and  $900^\circ\text{C}$ , the weight loss owing to evaporable water was negligible. The weight loss observed in the range  $400$ – $500^\circ\text{C}$  was attributed to the dehydroxylation of the portlandite. The differential scanning calorimetry (DSC) technique was used to study this feature in more detail.

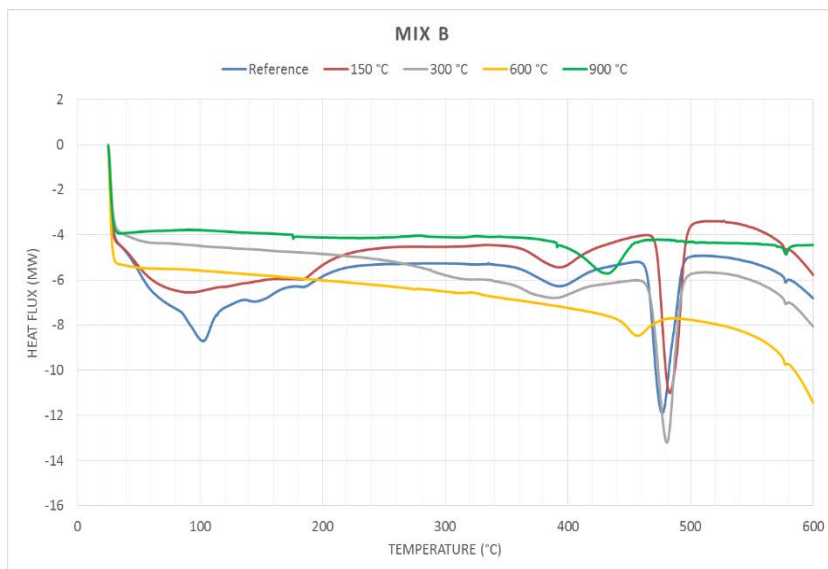
### 3.2 Differential scanning calorimetry (DSC)

The features observed in the DSC data for the samples depended as much on the heat treatment of the samples prior to analysis as on the samples themselves. A broad endotherm

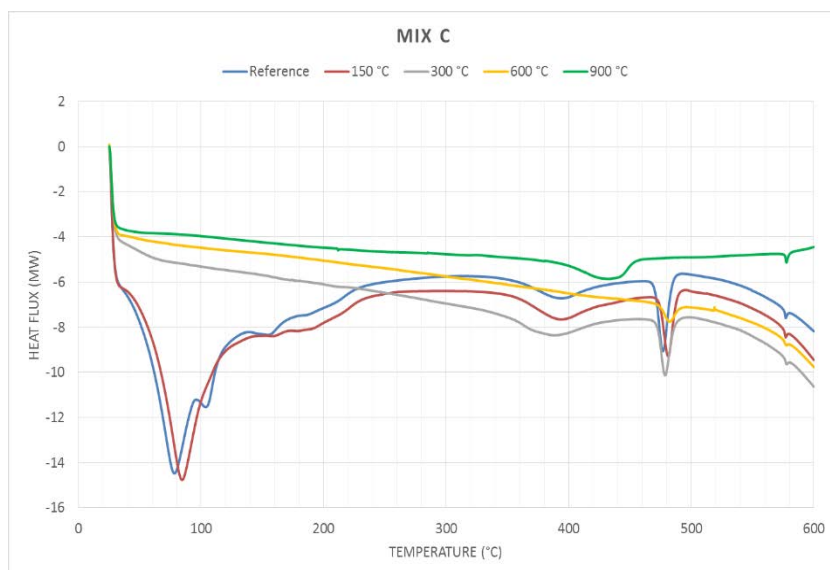
was observed between 40°C and 150°C for all samples pre-treated at  $\leq 150^\circ\text{C}$ , attributed to loss of water from the sample. This endothermic peak was substantially greater in Mix C due to the use of GGBS and SF as partial replacement materials of PC. The samples pre-heated to 300°C, 600°C and 900°C did not exhibit the same phenomenon in any of the three sample mixtures, as expected.



**Figure 4: Evolution of the Heat Flux vs Temperature, Mix A**



**Figure 5: Evolution of the Heat Flux vs Temperature, Mix B**



**Figure 6: Evolution of the Heat Flux vs Temperature, Mix C**

The DSC data across the temperature range 350°C to 500°C further reveals the alterations which have occurred across the concrete mixes. As noted above, this is the range in the TGA where a small weight loss occurred for samples which had undergone heat treatment <600°C. The DSC measurements, in this region are characterised by two endothermic peaks. The lower temperature peak (Feature 1 in Table 6), associated with the oxidation of iron hydroxides, was a broad feature and its onset was located at  $354^{\circ}\text{C} \pm 4^{\circ}\text{C}$  and varied insignificantly with the sample pre-treatment temperature. The enthalpy of the process however differed markedly with both mixture type and pre-treatment temperature. For Mix A, there was a decrease in the enthalpy, from  $12.1 \text{ J g}^{-1}$  for the reference sample to only  $4.92 \text{ J g}^{-1}$  for the 300°C sample. For the Mix B sample, the decrease in the enthalpy over this temperature range was less dramatic, from  $8.25 \text{ J g}^{-1}$  to  $6.06 \text{ J g}^{-1}$  respectively, whereas for Mix C, the enthalpy change was not significant.

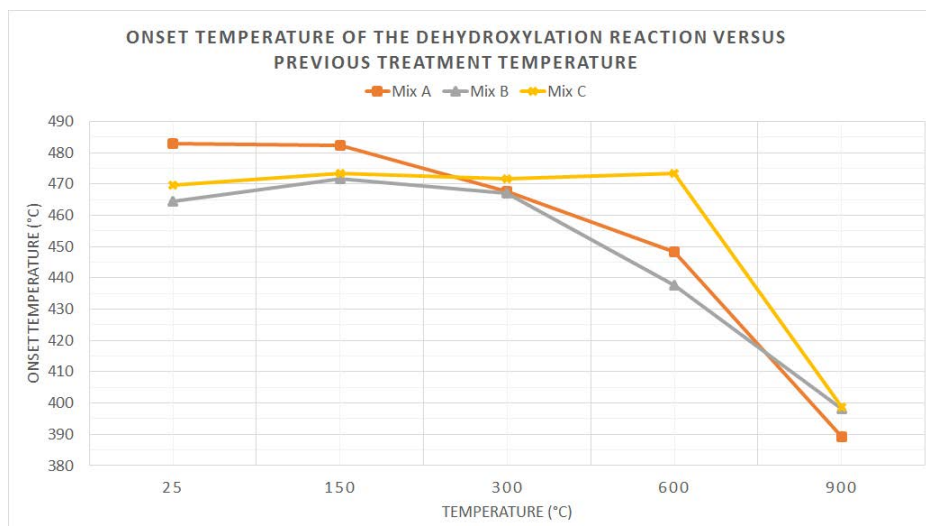
The higher temperature feature (Feature 2 in Table 6) is associated with the dehydroxylation of  $\text{Ca}(\text{OH})_2$ . This endothermic peak was much sharper and for Mix A and the onset temperature decreased from  $482^{\circ}\text{C}$  for the reference sample, to  $467^{\circ}\text{C}$  for the sample pre-treated at 300°C. More significantly, there was substantial increase in the enthalpy from  $15.3 \text{ J g}^{-1}$  to  $36.4 \text{ J g}^{-1}$ . For Mix B, no significant variations in onset temperature or indeed, in the enthalpy for the process ( $27.6 \pm 2.9 \text{ J g}^{-1}$ ) were observed whereas for Mix C, the enthalpy for the process was much lower ( $5.67 \pm 0.68 \text{ J g}^{-1}$ ). The relative changes in the enthalpies observed for Mix A, B and C are in line with the cementitious composition of the samples.

**Table 6: Onset Temperature and Enthalpy of Features 1 and 2 versus Previous Treatment Temperature**

Mix	Pre-treatment Temperature °C	Feature 1		Feature 2	
		$T_{\text{onset}}$ °C	Enthalpy J.g <sup>-1</sup>	$T_{\text{onset}}$ °C	Enthalpy J.g <sup>-1</sup>
A	25	358	12.10	482	15.30
	150	354	8.24	483	22.00
	300	353	4.92	467	36.40
	600	-	-	456	1.34
	900	-	-	389	9.48
B	25	355	8.25	464	27.40
	150	361	6.83	471	25.70
	300	353	6.06	466	29.80
	600	-	-	445	3.72
	900	-	-	374	13.80
C	25	349	8.78	470	6.46
	150	353	7.85	474	5.15
	300	348	9.50	471	5.40
	600	-	-	474	2.46
	900	-	-	394	9.03

The features which appear in the DSC data for samples pre-treated above 600°C are more revealing, *i.e.*, beyond the processes of oxidation of iron hydroxides, dehydroxylation of Ca(OH)<sub>2</sub>, quartz transformation and the decomposition of CaCO<sub>3</sub>. Here, the pair of peaks previously noted are now absent and a new broad feature appears [21, 22]. The onset temperature and enthalpy associated with this feature is strongly dependent on the sample pre-treatment temperature, as can be seen from the data in Table 6.

The peak shifts to lower temperature with increasing treatment temperature (Figure 7) but its enthalpy increases markedly for all the sample mixtures examined in the pre-treatment temperature range from 600°C to 900°C. The data suggests that the reformation of Ca(OH)<sub>2</sub> appears to become more facile in samples subjected to higher temperature treatment (900°C) and the subsequent dehydroxylation occurs at different temperatures compared to the untreated reference material.

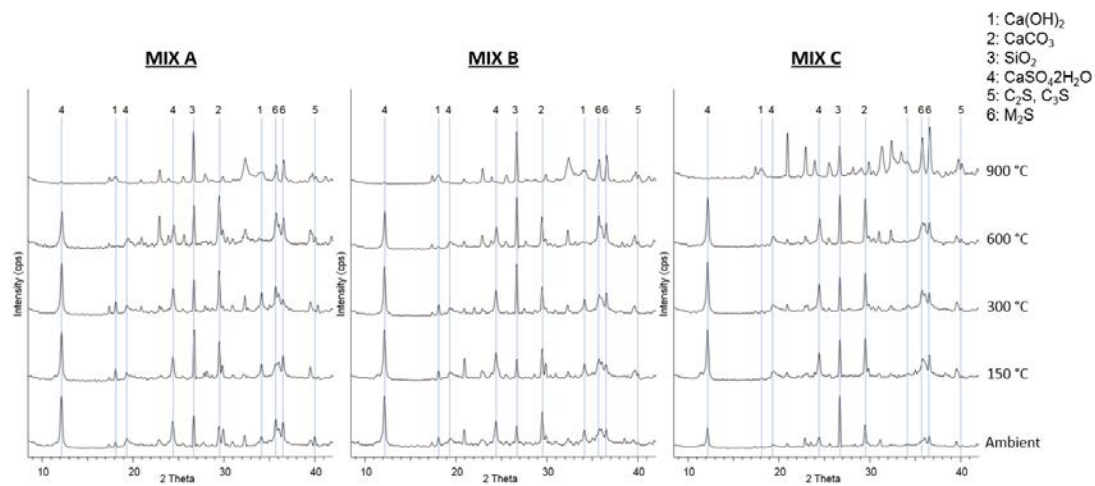


**Figure 7: Onset Temperature of the dehydroxylation reaction as a function of pre-treatment temperature**

From Figure 7, the onset temperature of thereformed portlandite decreased as the pre-heat temperature was increased. For Mix C, the onset temperature remained stable up to 600°C, thereafter it dropped notably from an average of 473°C to 394°C. The lowest onset temperature for samples pre-heated to 900°C was found for Mix A at 389°C. The heat flux at that temperature range reduced as the pre-heating temperature increased.

### 3.3 X-Ray Diffraction (XRD)

The effects of elevated temperatures on the mineralogical changes in the hydrated concrete matrix were studied by X-ray diffraction (XRD). The reference XRD pattern of all mixtures display peaks due to the presence of usual cement hydrated phases, such as portlandite, calcite, gypsum and C-S-H, as well as quartz from the aggregates in the concrete. Figure 8 shows the changes in XRD peaks with different heating regimes. The relative peak intensity of portlandite (peak 1) increased gradually with elevated temperature up to 300°C and then was eliminated at 600°C. The peak however reappears for a treatment temperature of 900°C for all the mixtures, albeit much less intense for Mix C. There are peaks related to Gypsum and Calcite (peaks 2 and 4) for all mixtures and for all treatment temperatures except for 900°C. These findings agree with the temperature range of calcite decomposition in the TGA curves and with the DSC data, as discussed above. Peaks related to quartz (peak 3) do not change with increasing temperature even though there is an  $\alpha$ - $\beta$  transition in quartz at 573°C. Alite (C<sub>3</sub>S), belite (C<sub>2</sub>S) and magnesium silicate (M<sub>2</sub>S) form during the dehydration process of the C-S-H gel (peaks 5 and 6).



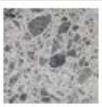
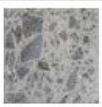




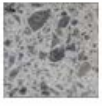











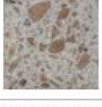





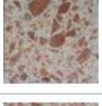
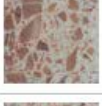




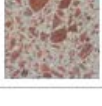





**Figure 8: X-ray diffractograms, Mixes A, B and C**

### 3.4 Macroscopic Observations

Visible colour change in concrete is the first indicator of potential deterioration and provides a relatively easy non-destructive approach for assessing damage. This discolouration is related to the characteristic chemical and physical changes of the cement paste and the aggregates [8]. The extent of this colour change is strongly dependant on the iron content of the concrete [21]. However, the transition of the colour of an aggregate from grey to red is influenced by its mineralogy. Gabbro stone consists primarily of plagioclase ( $\text{Ca}_{0.63}\text{Na}_{0.37}(\text{Al}_{1.63}\text{Si}_{2.37}\text{O}_8)$ ) and antigorite ( $\text{Mg}_3\text{Si}_2\text{O}_5(\text{OH})_4$ ), and has a low coefficient of thermal expansion, generally in the range  $5.5$  to  $8 \times 10^{-6}/^\circ\text{C}$ [22]. The colour observations are presented in Table 7.



**Table 7: Macroscopic observations, Mixes A, B and C**

Temperature (°C)	Polished cross section			Mortar surface			Relative Strength %		
	MIX A	MIX B	MIX C	MIX A	MIX B	MIX C	MIX A	MIX B	MIX C
25							100.0	100.0	100.0
150							88.5	95.6	102.9
300							120.0	117.7	119.3
600							93.4	98.0	119.3
900							18.0	20.6	19.3
1050							-	-	-

No changes were observed for temperatures up to 150°C and the concrete was still considered functional with the exception of Mix A, where the residual compressive strength had dropped to 88.5% of its strength at ambient temperature. Between 300°C and 600°C, the colour of the coarse aggregate and the mortar started to change to pinkish brown owing to oxidation of iron hydroxides. Some observations of thermal cracking due to volumetric growth and different expansion rates between the coarse aggregate and the mortar could be seen in that temperature range [23]. These changes may warrant further observation using other techniques.

The changes in colour were more obvious above 600°C and coincided with a dramatic loss of strength. The aggregate particles turned red and the cement paste became brownish in colour owing to the formation of CaO with the loss of CO<sub>2</sub> from CaCO<sub>3</sub>. The propagation of cracks became more obvious at this stage and contributed to a continuous weight loss. This observation agrees with the findings obtained using the TGA. The highest temperature reached during a fire incident within buildings is typically around 1050°C. When concrete specimens are exposed to this temperature, their surfaces become buff in colour and the concrete loses most of its strength leading to disintegration of its structure.

#### 4. Conclusions

A range of evaluation methods for fire exposed concrete have been presented including TGA, DSC, XRD and colour change. Mix C, containing GGBS and SF, demonstrated better resistance in terms of residual strength up to 600°C. Beyond that temperature, all mixtures lost most of their strength with complete disintegration occurring at high temperature (*ca.* 1050°C). The highest percentage of weight loss observed by thermogravimetry occurred in the region 700–900°C for all mixtures. This weight loss was mainly associated with the decomposition of calcium carbonates in the aggregates. It is possible that the degree of weight loss owing to that reaction may have been affected by the initial carbonation of the tested specimens. However, in this study, core samples were analysed and the depth of carbonation was negligible.

Two main regions were identified in the DSC data. The first was related to the breakdown of the gel-like C-S-H, while the second was associated with both the oxidation of iron hydroxides and the decomposition of the portlandite. Two events were found in the second region. For pre-treatment temperatures below 300°C, one was a broad endotherm at *ca.* 380°C and the second, a sharp endotherm at *ca.* 490°C. Above this pre-treatment temperature, only the higher temperature endotherm remained. The onset temperature for dehydroxylation of the reformed portlandite was determined from the DSC curves, and this was <400°C for all samples pre-heated to 900°C. This is a key finding as it provides valuable information for fire investigators during a scene reconstruction since it can be used as an indication of the maximum temperature reached during an incident.

A colour transformation in fire-affected areas is usually the first indicator of the extent of damage in concrete. Discolouration at high temperatures is related to the mineralogical changes that occur. The aggregate particles changed from grey to brown and then to red as the temperature increased. The reddish colour is caused by the oxidation of the iron hydroxides. This is in agreement with the XRD data obtained at the different temperatures. The trend of colour change in the mortar surface was not as significant, particularly with changing cement compositions. To study the effects of using cement substitutes on surface discolouration, colour meters or image analysis software packages may be utilised.

#### Acknowledgments

We are grateful to the Dubai Police GHQ for its grant support of this PhD project.

## References

1. Lin, W.-M., T. Lin, and L. Powers-Couche, *Microstructures of fire-damaged concrete*. ACI Materials Journal, 1996. **93**(3).
2. Ingham, J. *Forensic engineering of fire-damaged structures*. in *Proceedings of the ICE-Civil Engineering*. 2009. Ice Virtual Library.
3. Menéndez, E., C. Andrade, and L. Vega, *Study of dehydration and rehydration processes of portlandite in mature and young cement pastes*. Journal of thermal analysis and calorimetry, 2012. **110**(1): p. 443-450.
4. Georgali, B. and P.E. Tsakiridis, *Microstructure of fire-damaged concrete. A case study*. Cement and Concrete Composites, 2005. **27**(2): p. 255-259.
5. Hager, I., *Colour change in heated concrete*. Fire Technology, 2014. **50**(4): p. 945-958.
6. Annerel, E. and L. Taerwe, *Methods to quantify the colour development of concrete exposed to fire*. Construction and Building Materials, 2011. **25**(10): p. 3989-3997.
7. Short, N.R., J.A. Purkiss, and S.E. Guise, *Assessment of fire damaged concrete using colour image analysis*. Construction and Building Materials, 2001. **15**(1): p. 9-15.
8. Colombo, M. and R. Felicetti, *New NDT techniques for the assessment of fire-damaged concrete structures*. Fire Safety Journal, 2007. **42**(6-7): p. 461-472.
9. Arioz, O., *Effects of elevated temperatures on properties of concrete*. Fire Safety Journal, 2007. **42**(8): p. 516-522.
10. Annerel, E. and L. Taerwe, *Revealing the temperature history in concrete after fire exposure by microscopic analysis*. Cement and Concrete Research, 2009. **39**(12): p. 1239-1249.
11. Nijland, T.G. and J.A. Larbi, *Unraveling the temperature distribution in fire-damaged concrete by means of PFM microscopy: Outline of the approach and review of potentially useful reactions*. Heron, 2001. **46**(4): p. 253-264.
12. Alarcon-Ruiz, L., et al., *The use of thermal analysis in assessing the effect of temperature on a cement paste*. Cement and Concrete Research, 2005. **35**(3): p. 609-613.
13. Alonso, C. and L. Fernandez, *Dehydration and rehydration processes of cement paste exposed to high temperature environments*. Journal of materials science, 2004. **39**(9): p. 3015-3024.
14. Gabrovšek, R., T. Vuk, and V. Kaučič, *Evaluation of the hydration of Portland cement containing various carbonates by means of thermal analysis*. Acta Chim. Slov, 2006. **53**: p. 159-165.
15. Elchalakani, M., T. Aly, and E. Abu-Aisheh, *Sustainable concrete with high volume GGBFS to build Masdar City in the UAE*. Case Studies in Construction Materials, 2014. **1**: p. 10-24.
16. Abu Saleh, M., *Development of Sustainable and Low Carbon Concretes for the Gulf Environment*. 2014, University of Bath.
17. Harmathy, T. and N.R.C.C.D.o.B. Research, *Determining the temperature history of concrete constructions following fire exposure*. 1968: National Research Council Canada, Division of Building Research.
18. Handoo, S., S. Agarwal, and S. Maiti. *Application of DTA/TGA for the assessment of fire damaged concrete structures*. in *8th Proceedings National Symposium on Thermal analysis, Indian Thermal Analysis, Mumbai*. 1991.
19. Flick, E.W., *Handbook of adhesives raw materials*. 1989: William Andrew.
20. Ramachandran, V.S., et al., *Handbook of thermal analysis of construction materials*. 2002: William Andrew.
21. Gan, M., *Cement and concrete*. 1997: CRC Press.

22. Lamond, J.F. and J.H. Pielert, *Significance of tests and properties of concrete and concrete-making materials*. Vol. 169. 2006: ASTM International.
23. Rendell, F., R. Jauberthie, and M. Grantham, *Deteriorated concrete: inspection and physicochemical analysis*. 2002: Thomas Telford.